

Synthesis and characterization of aluminosilicates $[Zn_3(BTC)_2]$ hybrid composite materials

Nosheen AYUB

Ph. D. candidate at Fatima Jinnah Women University (FJWU) Rawalpindi Pakistan. She won International Research Support Initiative Program by Higher Education Commission, Pakistan and joined University of Glasgow, UK, to work under co-supervision of Prof. Duncan Gregory on Synthesis and characterization of composite materials research project. Her research interests are in exploring the potential of synthesized composite materials in different fields especially in electrochemistry and adsorption under supervision of Prof. Uzaira Rafique (Dean of Faculty of Sciences, FJWU).

Prof. Uzaira RAFIQUE

Dean of Faculty of Sciences at FJWU Rawalpindi Pakistan. His interests in research group lie in synthesis, structure and physical properties of inorganic, organic, hybrid and composite materials. The basic aim of the group is to discover new materials with potential useful properties particularly with projected applications in field of environmental remediation and sustainable development.

NOSHEEN AYUB • Department of Environmental Sciences, Faculty of Sciences, Fatima Jinnah Women University ▪ nosheen.ayub@gmail.com

UZAIRA RAFIQUE • Department of Environmental Sciences, Faculty of Sciences, Fatima Jinnah Women University

Érkezett: 2017. 10. 23. ▪ Received: 23. 10. 2017. ▪ <https://doi.org/10.14382/epitoanyag-jsbcm.2017.17>

Abstract

In this paper, hybrid composite materials based on metal organic framework $[Zn_3(BTC)_2]$ at aluminosilicates (zeolite) was explored for the first time. The composite was successfully synthesized by hydrothermal crystallization of zeolite followed by Solvothermal growth of $[Zn_3(BTC)_2]$ from its synthetic solution in the presence of dispersed zeolite particles. The synthesized materials were characterized by X-ray diffraction, Fourier transform infrared spectroscopy, scanning electron microscopy along with Energy dispersive X-ray spectrometric analysis. The XRD pattern exhibited the peaks characteristics of $[Zn_3(BTC)_2]$ in composite material. It meant that Zn-BTC represented the major component of the composites, and it also suggested that the composites preserved the crystalline characters of parent Zn-BTC. The results of FTIR and SEM/EDX further confirm the successful synthesis of composite hybrid material aluminosilicates with $[Zn_3(BTC)_2]$.

Keywords: Hybrid; zeolite; synthesis.

Kulcsszavak: Hibrid; zeolit; szintézis.

1. Introduction

Metal-organic frameworks (MOFs) are an emerging class of crystalline porous materials [1]. MOF consists of secondary building units, metal ions that act as lattice nodes, connected by organic linkers who impart high porosity and form modular structure [2]. Therefore by changing the connectivity of the inorganic moiety and nature of organic linker a wide structural diversity and highly designable pore sizes and shapes in MOFs are expected, which endow MOFs with tunable cavity architectures and properties. MOFs are synthesized both traditional and rather specific methods like use of microwave, ultrasonic, mechanochemical and electrochemical processing [3]. The reproducibility of the results of synthesis and post synthetic treatment of the produced samples is of critical importance. MOFs are most often functionalized to make them appropriate for precise application. In current era, the possibility to vary the structure porosity, topology and elemental composition (the Al:Si ratio and isomorphous substitution of transition metal atoms in tetrahedral positions) has rendered zeolites and their derivatives the most suitable materials for use in a variety of applications: in gas adsorption and separation, catalysis, photocatalysis. Zeolites and their derivatives have been addressed in experimental and theoretical studies.

However, MOFs are superior to zeolites in various respects; in specific, a characteristic feature of MOFs is the large surface area. Metal-organic frameworks vary from zeolites in numerous key aspects. The key change of the MOFs is an extensive diversity and variability of their structure in combination with lower topological restrictions on the formation of porous three-dimensional frameworks. A significant number of new MOF structures synthesized every year confirms this variability

and heightened interest in their potential application areas. Zeolites are built of tetrahedral fragments, and differences in their topology are based on a finite number of secondary structure elements, whereas inorganic secondary building units of MOFs can be both a separate metal atom or a more or less complicated cluster and one, two or three-dimensional extended inorganic substructures.

Nevertheless thermal stability of zeolite is higher than MOF. So, Assimilation of MOFs with different functional materials is a very effective and viable approach to further improve MOF performance [4] or present innovative functionality for practical use [5]. Thus far, various MOF composites have been fruitfully prepared by assembling MOFs and functional species, including graphene, carbon nanotubes (CNTs), metal oxides, complexes, and have shown remarkable performance in catalysis [6], photo-induced H_2 generation [7], proton conduction [8], and so on. In these MOF composites, the individual functions of the MOFs and functional materials synergistically fuse together not only to deliver multifunctionality as a whole but also to produce new physical and chemical properties that are not present in the individual components [9]. The combination of MOFs and other functional materials has extended their applications. Moreover, research on high-performance MOF hybrids with sophisticated architectures, in combination with enrichment of the MOF database, has led to new design tactics for MOF composites.

In this study, we report the synthesis of zeolite-MOF composite materials by Solvothermal growth of MOF on the surface of zeolite. Zeolite-MOF composite has the potential to be novel and useful porous system the variety of application, as the inorganic zeolite component imparts the advantages of their higher thermal, mechanical and structural stability

and the organic MOF imparts specific functionality and high flexibility.

2. Experimental

2.1. Materials

Analytical grade reagents, such as aluminumisopropoxide, sodium hydroxide (NaOH), tetraethyl ammonium hydroxide (TEAOH), Tetraethylorthosilicate (TEOS), Ammonium nitrate (NH_4NO_3), 1,3,5-benzenetricarboxylic acid or trimesic acid (TMA), zinc nitrate hexahydrate ($\text{Zn}(\text{NO}_3)_2 \cdot 6\text{H}_2\text{O}$), methanol (CH_3OH) and N-N-dimethylformamide (DMF) were purchased from commercial source (Sigma-Aldrich) and used without further purification.

2.2. Synthesis

2.2.1. Synthesis of aluminosilicates (Zeolite)

The method to synthesis of zeolite was modified from literature [10]. The synthesis mixture was prepared as follows: NaOH aqueous solution (1 M), TEAOH solution (5 mL) and aluminumisopropoxide (0.1 g) were mixed and stirred until all components were dissolved. At last silica source, TEOS (6 ml) was added in above solution and stirred for an additional 30 min before crystallization to get a homogenous gel. Later on this gel was transferred to a stainless steel autoclave and placed in furnace at 150 °C for 24 h at heating rate of 10 °C/min. After completion of the reaction autoclave was cooled down to room temperature and product obtained was collected by centrifugation at 4000 rpm for 15 min. The synthesized material was washed with deionized water before drying overnight at 50°C and calcined in furnace at 600 °C for 6 h. Calcined zeolite was protonated by ion-exchange with 1.0 M NH_4NO_3 solution, stirred at 80 °C for 2 h. The solid was filtered, washed with distilled water and dried at 50 °C overnight. The solid powder was then calcined at 550 °C at the rate of 5 °C/min for 4 h in order to remove NH_3 for the generation of zeolite in H^+ form.

2.2.2. Synthesis of $[\text{Zn}_3(\text{BTC})_2]$

$[\text{Zn}_3(\text{BTC})_2]$ was synthesized using Solvothermal method [11]. The procedure was as follow: 0.368 g of zinc nitratehexahydrate ($\text{Zn}(\text{NO}_3)_2 \cdot 6\text{H}_2\text{O}$) was dissolved in 20 mL of DMF: CH_3OH : H_2O (1:1:1 v/v). The quantity of 0.148 g of 1, 3, 5-benzenetricarboxylic acid was dissolved in 20 mL of the same solvent mixture and both solutions were combined with stirring. The resulting mixture was transferred to Teflon-lined stainless steel autoclave and placed in furnace at 150 °C for 24 h. At the end of the reaction, the autoclave was cooled down to room temperature, and the resulting white powder was washed with the same solvent mixture and dried overnight at 60 °C.

2.2.3. Synthesis of aluminosilicate $[\text{Zn}_3(\text{BTC})_2]$ nanocomposite

The synthesis of zeolite- $[\text{Zn}_3(\text{BTC})_2]$ composite was performed by the same procedure described above except that 0.1 g zeolite particles of the procedure 2.2.1 were added to the synthetic solution of $[\text{Zn}_3(\text{BTC})_2]$ prior to Solvothermal crystallization of MOF.

2.3. Characterization

2.3.1. Powder X-ray diffraction XRD

X-ray diffraction (XRD) measurements were done with Cu K α radiation ($\lambda=1.5418\text{\AA}$, 40 kV, 40 mA). The powder samples were ground and spread on a sample holder. The samples were scanned in the range from $2\theta=5^\circ-50^\circ$ with a step size of 0.0334°.

2.3.2. Fourier Transform Infrared Spectroscopy FTIR

FTIR technique was used for the determination of functional groups in synthesized materials in transmittance (%) mode with a 16 cm^{-1} resolution and 50 scans in the mid IR region (400–4000 cm^{-1}).

2.3.3. Scanning electron microscopy/Energy dispersive X-ray sepectroscopy SEM/EDX

The morphology of the prepared materials was examined on scanning electron microscope (SEM) along with EDX.

3. Result and Discussion

Zeolite, $[\text{Zn}_3(\text{BTC})_2]$ and zeolite- $[\text{Zn}_3(\text{BTC})_2]$ were successfully synthesized using Solvothermal method. Synthesis of zeolite- $[\text{Zn}_3(\text{BTC})_2]$ was carried out by hydrothermal crystallization of zeolite followed by Solvothermal growth of $[\text{Zn}_3(\text{BTC})_2]$ from its synthetic solution in the presence of dispersed zeolite particles.

Fig. 1 shows XRD pattern of zeolite, $[\text{Zn}_3(\text{BTC})_2]$ and zeolite- $[\text{Zn}_3(\text{BTC})_2]$. The reflection peaks in XRD pattern of zeolite are consistent with those reported for the topologies of zeolite material. The peaks between 10° and 20° are related to cubic crystalline structure of $[\text{Zn}_3(\text{BTC})_2]$, which is in good agreement with that reported in literature [12,13], suggesting that $[\text{Zn}_3(\text{BTC})_2]$ was successfully synthesized by Solvothermal method.

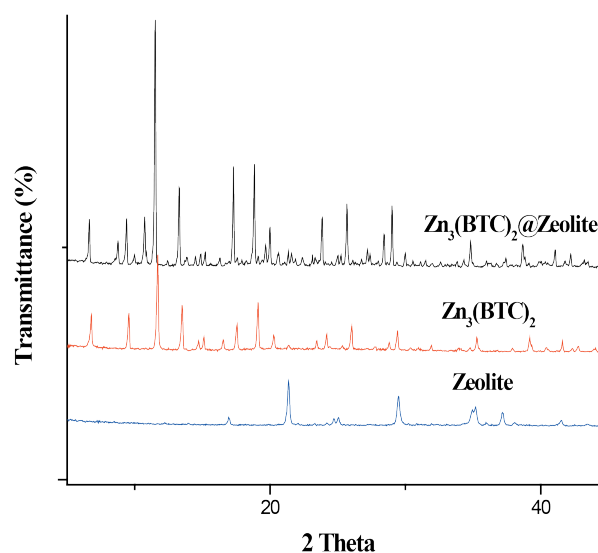


Fig. 1. XRD pattern of Zeolite, $\text{Zn}_3(\text{BTC})_2$, and Zeolite- $\text{Zn}_3(\text{BTC})_2$
1. ábra Zeolit, $\text{Zn}_3(\text{BTC})_2$ és Zeolit- $\text{Zn}_3(\text{BTC})_2$ röntgendiffraktogramjai

In XRD pattern of zeolite- $[\text{Zn}_3(\text{BTC})_2]$ the main peak of $[\text{Zn}_3(\text{BTC})_2]$ is at 11.5° is not changed after modification. It meant that Zn-BTC represented the major component of the

composites, and it also suggested that the composites preserved the crystalline characters of parent Zn-BTC. The similar pattern of XRD for composite material indicates the existence of well-defined MOF units in the synthesis materials. Thus, one can assume that zeolite did not prevent the formation of linkage between the zinc dimer and organic ligand [14].

FTIR spectra further confirm the results of XRD analysis on the formation of zeolite, $[\text{Zn}_3(\text{BTC})_2]$ and composite material. It can obviously see that all vibration bands of IR spectra of zeolite and those for $[\text{Zn}_3(\text{BTC})_2]$ were in good agreement with the published data [13]. All the characteristic peaks of zeolite could be observed in zeolite- $[\text{Zn}_3(\text{BTC})_2]$ composite, indicating that hybrid composites were successfully synthesized, being mainly composed of zeolite and $[\text{Zn}_3(\text{BTC})_2]$.

Fig. 2 represents the FTIR spectra of the synthesized materials. For zeolite, the characteristic broad features at 958 cm^{-1} were the asymmetric stretching vibration of T-O-T (T: Si or Al) in the framework of zeolite. For $[\text{Zn}_3(\text{BTC})_2]$, the five typical bands were almost identical with those for the zeolite- $[\text{Zn}_3(\text{BTC})_2]$ composites, indicating that MOF played major role in the hybrid composites. Another characteristic peaks are placed at 453 and 552 cm^{-1} for Zn (II) which prove the bonding between metal and carboxylic oxygen. The vibration bands centered on $1621/1562\text{ cm}^{-1}$ and $1433/1364\text{ cm}^{-1}$ correspond to the asymmetric stretching and the symmetric stretching vibrations of carboxylate groups respectively [12]. The presence of strong stretching vibration peak at 1621.17 cm^{-1} confirmed the deprotonation of carboxylate groups in 1, 3, 5-benzenetricarboxylic acid, upon reaction with metal ions [15].

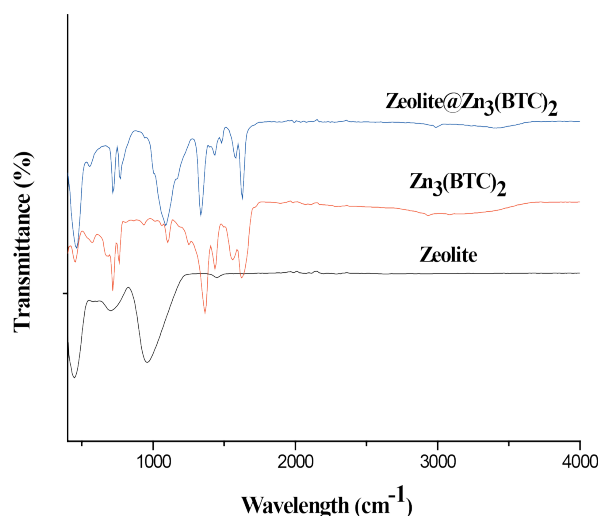


Fig. 2. FTIR spectrum of Zeolite, $\text{Zn}_3(\text{BTC})_2$ and Zeolite- $\text{Zn}_3(\text{BTC})_2$
2. ábra Zeolit, $\text{Zn}_3(\text{BTC})_2$ és Zeolit- $\text{Zn}_3(\text{BTC})_2$ FTIR spektrumai

From Fig. 3, the SEM photographs revealed the morphologies of the zeolite, $\text{Zn}_3(\text{BTC})_2$ and composite material. Compared with pure $\text{Zn}_3(\text{BTC})_2$, the composite particles (Fig. 3.c) still remain in its pure shape indicating an intact host matrix after loading the sample with zeolite.

EDX spectrum was shown in Fig. 4. Spectrum (Fig. 4.a) was of the zeolite particles. The zeolite construction element Si, Al and O were shown in the figure with $\text{K}\alpha$ characteristic X-ray energy of 1.739 KeV , 1.486 KeV and 0.525 KeV , indicating the

presence of zeolite particles. The EDX spectrum (Fig. 4.c) was of composite particles and was comprised of Si, Al, O and Zn peaks, indicating the presence of zeolite and MOF structures. The primary construction element of $[\text{Zn}_3(\text{BTC})_2]$ Zn was shown with $\text{L}\alpha$ characteristic X-ray energy of 1.042 KeV . The peaks at 0 come from the X-ray beam of the instrument. The EDX was done during the SEM and was performed on isolated particles, thus confirms the successful growth of zeolite onto $[\text{Zn}_3(\text{BTC})_2]$ and the preservation of the crystallinity of both materials.

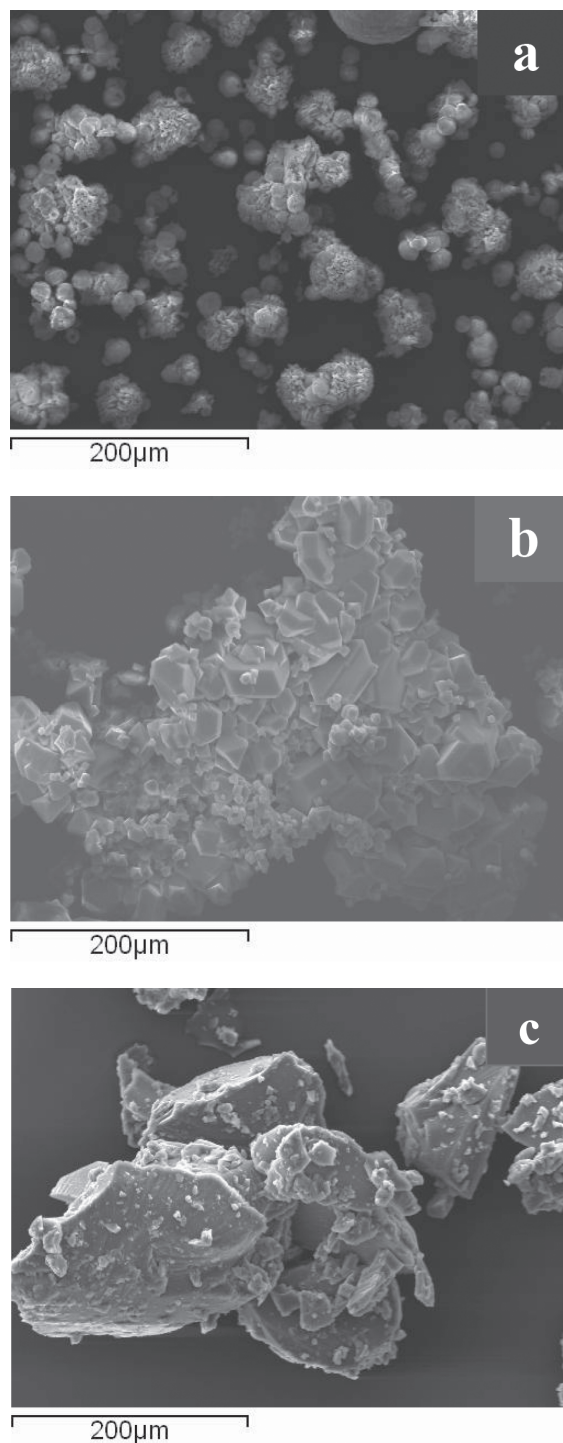


Fig. 3. SEM photograph of (a) Zeolite, (b) $\text{Zn}_3(\text{BTC})_2$ and (c) Zeolite- $\text{Zn}_3(\text{BTC})_2$
3. ábra Zeolit, $\text{Zn}_3(\text{BTC})_2$ és Zeolit- $\text{Zn}_3(\text{BTC})_2$ elektronmikroszkóp felvételei

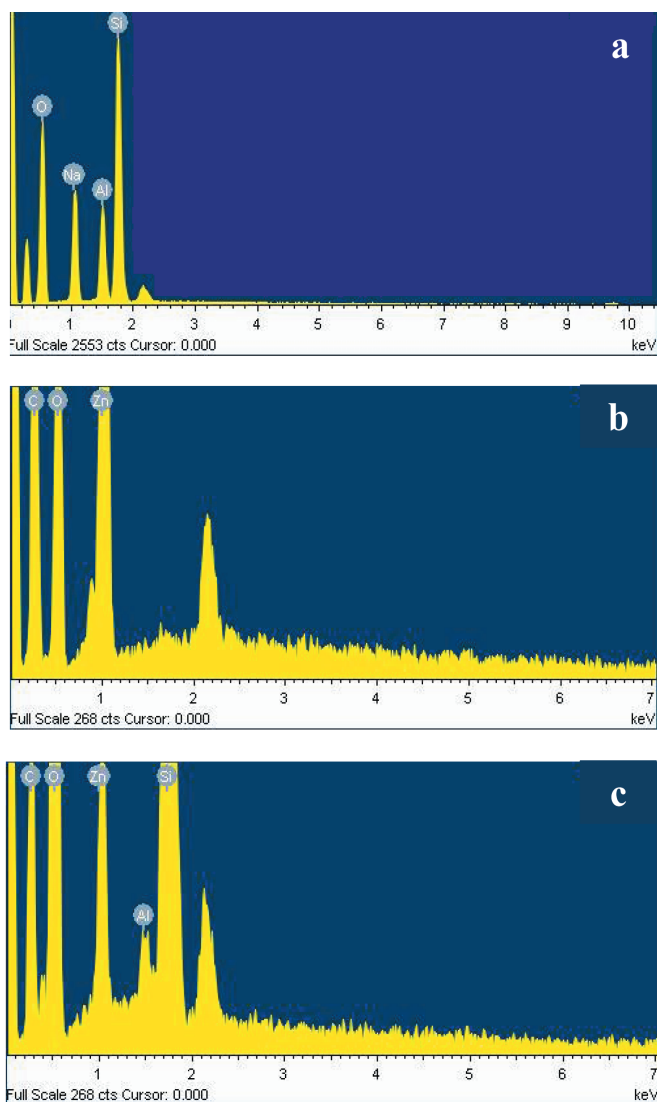


Fig. 4. EDX spectrum of (a) Zeolite, (b) $Zn_3(BTC)_2$ and (c) Zeolite- $Zn_3(BTC)_2$
 4. ábra Zeolit, $Zn_3(BTC)_2$ és Zeolit- $Zn_3(BTC)_2$ EDX spektrumai

Conclusions

In summary, we report the synthesis of porous co-ordination network of $Zn_3(BTC)_2$ by solvothermal growth upon zeolite particles which were pre-synthesized via hydrothermal crystallization. The physiochemical and texture properties of synthesized materials were confirmed by XRD, FTIR and SEM/EDX. In XRD pattern of composite material (aluminosilicates with $[Zn_3(BTC)_2]$) the main peak of $[Zn_3(BTC)_2]$ is at 11.5° which is not changed after modification. It meant that Zn-BTC represented the major component of the composites, and it also suggested that the composites preserved the crystalline characters of parent Zn-BTC. The co-existence of both vibrational peaks of zeolite and $[Zn_3(BTC)_2]$ in FTIR results further confirms the synthesis of composite material. SEM images of pure $[Zn_3(BTC)_2]$ and composite material shows that the composite particles still remain in its parent shape indicating an intact host matrix after loading the sample with zeolite. EDX results further confirm the successful synthesis of composite and strengthen the results of XRD, FTIR and SEM.

References

- [1] Zhou, H. C. – Long, J. R. – Yaghi, O. M. (2012): Introduction to metal-organic frameworks, *Chemical Reviews*, Vol. 112, No. 2, pp. 673-674. <https://doi.org/10.1021/cr300014x>
- [2] Allendorf, M. D. – Stavila, V. (2015): Crystal engineering, structure-function relationships, and the future of metal-organic frameworks. *Crystal Engineering Communication*, Vol. 17, No. 2, pp. 229-246. <https://doi.org/10.1039/C4CE01693A>
- [3] Butova, V. V. E. – Soldatov, M. A. – Guda, A. A. – Lomachenko, K. A. – Lamberti, C. (2016): Metal-organic frameworks: structure, properties, methods of synthesis and characterization. *Russian Chemical Reviews*, Vol. 85, No. 3, pp. 280-307. <https://doi.org/10.1070/RCR4554>
- [4] Wang, C. – Liu, D. – Lin, W. (2013): Metal-organic frameworks as a tunable platform for designing functional molecular materials. *Journal of the American Chemical Society*, Vol. 135, No. 36, pp. 13222-13234. <https://doi.org/10.1021/ja308229p>
- [5] Q.-L. Zhu – Q. Xu (2014): Metal-organic framework composites. *Chemical Society Reviews*, Vol. 43, pp. 5468-5512. <https://doi.org/10.1039/C3CS60472A>
- [6] Q.-L. Zhu – Q. Xu (2016): Immobilization of ultrafine metal nanoparticles to high-surface-area materials and their catalytic applications. *Chem*, Vol. 1, pp. 220-245. <http://dx.doi.org/10.1016/j.chempr.2016.07.005>
- [7] C. Wang – K. E. de Krafft – W. Lin (2012): Pt nanoparticles@photoactive metal-organic frameworks: efficient hydrogen evolution via synergistic photoexcitation and electron injection. *Journal of the American Chemical Society*, Vol. 134, pp. 7211-7214. <http://dx.doi.org/10.1021/ja300539p>
- [8] P. Ramaswamy – N. E. Wong – G. K. H. Shimizu (2014): MOFs as proton conductors-challenges and opportunities, *Chemical Society Reviews*, Vol. 43, pp. 5913-5932. <http://dx.doi.org/10.1039/C4CS00093E>
- [9] Kitao, T. – Zhang, Y. – Kitagawa, S. – Wang, B. – Uemura, T. (2017): Hybridization of MOFs and polymers, *Chemical Society Reviews*, Vol. 46, pp. 3108-3133. <http://dx.doi.org/10.1039/C7CS00041C>
- [10] Baradaran, S. – Sohrabi, M. – Bijani, P.M. – Javid, S. (2015): The 15th Iranian National Congress of Chemical Engineering, *University of Tehran*, Tehran, Iran, 17-19 February 2015.
- [11] Thi, T. V. N. – Luu, C.L. – Hoang, T. C. – Nguyen, T. – Bui, T. H. – Nguyen, P. H. D. – Thi, T. P. P. (2013): Synthesis of MOF-199 and application to CO_2 adsorption, *Advances in Natural Sciences: Nanoscience and Nanotechnology*, Vol. 4, No. 3, 035016. <https://doi.org/10.1088/2043-6262/4/3/035016>
- [12] Abbasi, A. R. – Noori, N. (2014): Synthesis, Characterization and Antibacterial Properties of Nano-Porous $Zn_3(BTC)_2 \cdot 12H_2O$ upon Silk Yarn Under Ultrasound Irradiation. *Journal of Inorganic and Organometallic Polymers and Materials*, Vol. 24, No. 6, pp. 1096-1102. <https://doi.org/10.1007/s10904-014-0101-5>
- [13] Yang, Q. – Zhang, M. – Song, S. – Yang, B. (2017): Surface modification of PCC filled cellulose paper by MOF-5 ($Zn_3(BDC)_2$) metal-organic frameworks for use as soft gas adsorption composite materials. *Cellulose*, Vol. 24, No. 7, pp. 1-10. <https://doi.org/10.1007/s10570-017-1331-9>
- [14] Petit, C. – Burrell, J. – Bandosz, T. J. (2011): The synthesis and characterization of copper-based metal-organic framework/graphite oxide composites. *Carbon*, Vol. 49, No. 2, pp. 563-572. <https://doi.org/10.1016/j.carbon.2010.09.059>
- [15] Papageorgiou, S. K. – Kouvelos, E. P. – Favvas, E. P. – Sapidis, A. A. – Romanos, G. E. – Katsaros, F. K. (2010): Metal-carboxylate interactions in metal-alginate complexes studied with FTIR spectroscopy, *Carbohydrate Research*, Vol. 345, No. 4, pp. 469-473. <https://doi.org/10.1016/j.carres.2009.12.010>

Ref.:

Ayub, Nosheen – Rafique, Uzaira: *Synthesis and characterization of aluminosilicates $[Zn_3(BTC)_2]$ hybrid composite materials*
 Építőanyag – Journal of Silicate Based and Composite Materials,
 Vol. 69, No. 3 (2017), 98–101. p.
<https://doi.org/10.14382/epitoanyag-jsbcm.2017.17>